Available online at www.sciencedirect.com
ScienceDirect
C. R. Chimie 13 (2010) 40–51
Comptes Rendus Chimie

Account / Revue

Design of metal oxide nanoparticles: Control of size, shape, crystalline structure and functionalization by aqueous chemistry

Jean-Pierre Jolivet *, Sophie Cassaignon, Corinne Chanéac, David Chiche, Olivier Durupthy, David Portehault

LCMC, UMR-CNRS 7574, université Pierre-et-Marie-Curie–Paris 6, Collège de France, 11, place Marcelin-Berthelot, 75231 Paris cedex 05, France

Received 3 April 2009; accepted after revision 18 September 2009
Available online 12 January 2010

Abstract

The aim of this paper is to show that a very simple but well controlled chemistry in an aqueous medium allows one to efficiently control the main characteristics of oxide nanoparticles. Examples concerning titania, alumina, iron and manganese oxides are discussed to illustrate various effects on the control of size, shape and structure of nanoparticles. Some examples of functionalization of these particles are also illustrated. Experimental data, procedures and detailed references can be found in the cited literature. ***To cite this article: J.-P. Jolivet et al., C. R. Chimie 13 (2010).***

Résumé

Cet article a pour but de montrer qu'une chimie en milieu aqueux très simple mais bien maîtrisée permet de contrôler efficacement les principales caractéristiques des nanoparticules d'oxydes métalliques. Des exemples concernant les oxydes de titane, d'aluminium, de fer et de manganèse sont discutés pour illustrer divers effets sur le contrôle de la taille, la forme et la structure cristalline des nanoparticules. Quelques exemples de fonctionnalisation de ces particules sont aussi présentés. Les données expérimentales, procédures et références détaillées sont incluses dans la littérature citée. ***Pour citer cet article : J.-P. Jolivet et al., C. R. Chimie 13 (2010).***

Keywords: Oxide nanoparticles; Precipitation; Aqueous chemistry of metal cations; Surface energy; Titania; Aluminium oxide; Manganese oxides; Aggregation; Oriented attachment; Heterogeneous nucleation

Mots clés : Nanoparticules d'oxyde ; Précipitation ; Chimie aqueuse ; Chimie des cations ; Énergie de surface ; Oxydes de titane ; Oxydes d'aluminium ; Oxydes de manganèse ; Agrégation ; Attachement orienté ; Nucléation hétérogène

1. Why the design of nanoparticles?

Nanotechnologies are based on specific properties of ultradivised matter in optics, photonics, electronics or magnetism, resulting from a mean size of particles or

* Corresponding author.
E-mail address: jean-pierre.jolivet@upmc.fr (J.-P. Jolivet).

1631-0748/$ – see front matter
doi:10.1016/j.crci.2009.09.012

domains of size similar to those of characteristic lengths of physics (mean free path of electron, wavelength of light, size of magnetic domains...) [1]. Specific properties are also due to the huge specific area of nanoparticles enabling their dispersion within composites or giving a high surface reactivity for catalysts. Optimization of the performances of nanomaterials needs, however, a careful control of many characteristics (size, shape, crystalline structure for polymorph materials, dispersion state, surface state...) on which depend their properties. In addition, fabrication of nanomaterials has to be cheap, easy and environmentally friendly by involving green chemistry. There is a lot of processes in solution to obtain nanosystems with controlled characteristics, the more often involving organometallic precursors, non-aqueous medium and/or the use of surfactant molecules and various organic additives to constrain size or shape of nanomaterials [2]. We show that aqueous chemistry of metal cations and oxides allows one, in many cases, to control very easily and, in a green chemistry context, the design of metal oxide nanoparticles. Some technologically interesting materials such as magnetic iron oxides, alumina, titanium and manganese dioxides will be considered. These results have been obtained in our research team belonging to Jacques Livage's lab in Paris. We are happy to illustrate the ''Chimie douce'' concept introduced by Jacques and we thank him as friends for his contribution in this field.

2. Ultra divided solids? A problem of surface energy to control particle size

The surface energy represents always a positive component to the free enthalpy of a dispersed system. The other component represents the negative bulk energy. Let us consider particles in formation from molecular complexes in solution. If particles are growing with a high surface energy, the system spontaneously tends to decrease the interface solid-solution area and particles tend to grow in order to minimize the surface energy. If the surface energy is very low, there is practically no energetic penalty to create surface and very small particles can be stable in dispersion. In fact, the surface energy of particles in suspension can be decreased by adsorption, as expressed by Gibbs's law giving the effect of adsorption on the interfacial tension γ, $d\gamma = -\Gamma_i d\mu_i$ (Γ_i is the adsorption density of the i species under the chemical potential μ_i). Many adsorbed species can be involved, especially the proton in aqueous medium. In effect, the acidity of the medium of synthesis strongly influences the particle size for many oxides and hydroxides. The Fig. 1 shows size effects observed with magnetite Fe_3O_4, anatase TiO_2 and brucite $Mg(OH)_2$ [3].

In all these cases, precipitation occurred in carefully controlled conditions where the pH of the medium was kept at a constant value during precipitation. Such an effect of acidity on the particle size has been semi-quantitatively evaluated, taking into account the electrostatic surface charge density (σ) due to proton adsorption-desorption and its impact on interfacial tension. In fact, on each side of the point of zero charge (PZC) where σ is positive or negative, the surface energy is lowered by a change in chemical composition. An increase of area and consequently a decrease of particle size (increase of surface to volume ratio) are then favored when the pH of synthesis is kept far from the PZC of the material during its precipitation. The Fig. 2 shows the experimental and calculated variations of charge density, interfacial tension and particle size according to the model described in [3] for magnetite nanoparticles.

For isotropic particles (pseudo-spherical particles exposing faces of a same type), the shape is the same when the size changes, while for anisotropic particles significantly different types of faces are present, each with its own structure and reactivity and a change in

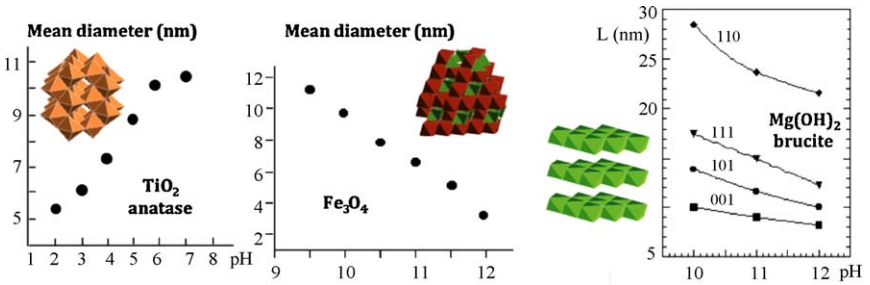

Fig. 1. Variation of particle diameter with the pH of precipitation for anatase (aged for one week at 60 °C) and magnetite (aged for one week at 25 °C), and apparent dimensions deduced from XRD line broadening for brucite (aged for two weeks at 60 °C).

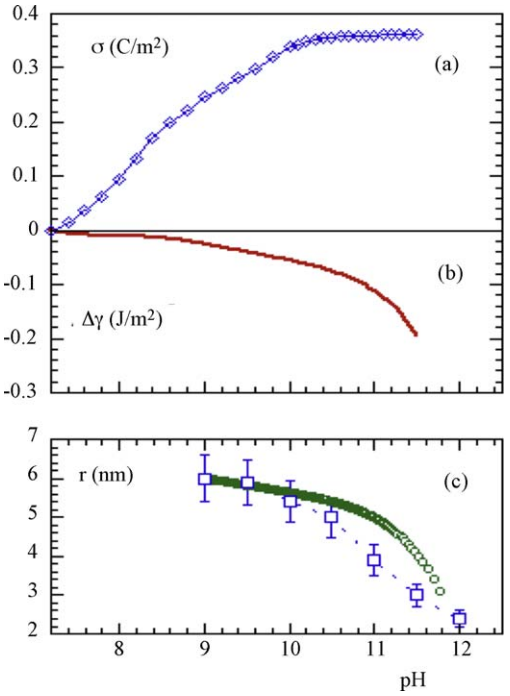

Fig. 2. a: experimental variation of the surface charge density of magnetite particles as a function of the pH; b: calculated variation of the interfacial tension; c: experimental (□) and (o) calculated variation of the mean particle diameter.

surface energy leads to a change in morphology (see later).

The effect of acidity on particle size seems to be of thermodynamic rather than kinetic origin (practically no Ostwald's ripening occurs when the particles are synthesized far from the PZC) [3]. This phenomenon appears to be very similar to the formation of microemulsions by adding surfactant into an oil-water mixture. In this last case, true thermodynamically stabilized dispersions are formed because the adsorption of surfactant molecules at the water-oil interface reduces the interfacial tension up to very low values (10^{-3}–10^{-4} Jm^2) [4].

It is interesting to observe that the control of particle size by acidity keeps ''clean'' oxide surfaces without foreign species adsorbed. This is important especially for magnetic nanomaterials such as spinel iron oxide nanoparticles. With controlled variable size and different surface to volume ratios, these nanoparticles were well designed for the study of their magnetic properties, especially surface effects and magnetic interactions by avoiding perturbations in surface magnetism often encountered when adsorbed additives are used for the control of particle size [5]. Anatase was also well designed to study the influence of particle size on Raman spectra using a model of phonon confinement in nanoparticles [6].

3. Control of crystalline structure of oxide nanoparticles

With polymorphic solids, it is possible to synthesize selectively one or other of the crystalline forms by controlling different parameters. The nature of the coordination sphere of the precursor can be modified by specific ligands to orient the condensation process. It is also possible to work with different conditions of solubility of the solid in order to involve different crystallization processes, typically crystallization *in situ* in the solid state or dissolution-crystallization of a preexistent amorphous or metastable phase. If an element exists under different oxidation states, it is also possible to transform a preexistent solid phase by a redox process. All these processes are well exemplified by the chemistry of titanium, manganese and iron.

Titania, TiO_2, mainly exists as three polymorphs, namely anatase, brookite and rutile, following increasing thermodynamic stability. These three forms can be obtained quasi selectively from the same soluble precursor, $TiCl_4$, in well-controlled conditions in which different mechanisms are at work. Addition of a base into a solution of $TiCl_4$ at a pH in the range 2 to 7 instantaneously forms an amorphous precipitate which evolves to anatase by aging for 24 hours at 60 °C [3]. The solubility of titanium in these acidity conditions is very low and no change in particle size was observed during aging, showing that crystallization proceeds by dehydration and structuration *in situ* of the early amorphous solid phase. In such conditions, anatase is formed because it is the less thermodynamically stable phase among the different polymorphs, with the lowest interfacial tension. As shown before, roughly spherical particles are obtained and the particle size is depending on the pH of precipitation because the surface energy is directly correlated to the surface charge density.

When a solution of $TiCl_4$ strongly acidified by a non complexing acid such as perchloric acid is heated around 100 °C for some days, nanorods of rutile are progressively obtained [7]. In such conditions, the three polymorphs are initially simultaneously formed in variable proportions but the dissolution-crystallization process transforms the less thermodynamically stable phases, anatase and brookite, into rutile. The length of rutile nanorods increases when the acidity and the duration of thermolysis increase, confirming that dissolution-crystallization process is working. The aspect ratio of nanoparticles can so easily tuned from

around 5 up to 15. Small rods exhibit original properties such as electrochemical intercalation of lithium forming reversibly a rutile-type Li_xTiO_2 phase with x varying from 0 to 0.5. For $x > 0.5$, the rock-salt $LiTiO_2$ phase is obtained. The small size of particles enables an increase up to 10% in volume of the crystal cell while intercalation does not significantly occur in massive rutile particles [8]. Needles and long rods of rutile nanoparticles (aspect ratio ≥ 15) in concentrated aqueous dispersion spontaneously form a phase exhibiting a nematic liquid crystal behavior. These dispersions can be used to form solid films supported onto glass slides, in which the particles keep their orientation. Such oriented thin films have photocatalytic properties, evidenced by degradation of methylene blue under UV irradiation, that are depending on the relative orientations of the film and of the polarization of UV light [9].

Thermolysis around 100 °C of solutions of $TiCl_4$ strongly acidified by chlorhydric acid (1 to 6 mol.L^{-1} in HCl) forms brookite and rutile nanoparticles, with relative proportions strongly depending on the acidity [7]. In fact, the nature of the solid phase is rather depending on the chloride to titanium molar ratio, because it determines the speciation of early soluble complexes of titanium. So, when the composition of the medium corresponds to the predominance of the neutral complex $[Ti(OH)_2Cl_2(OH_2)_2]$, around 80% of the solid are nanoplatelets of brookite, suggesting this species is the precursor of brookite. The presence of two chloride ligands in the coordination sphere of the precursor orients the condensation steps allowing the crystallization of brookite preferentially. The role of chloride on crystallization of brookite is confirmed by the fact that when the brookite nanoparticles so obtained are thermolyzed in perchloric acid solution, transformation into rutile occurs quickly, while if chloride ions are introduced at the adequate concentration into the acidic medium before heating, brookite particles do not evolve [7]. Brookite may also be obtained by thermolysis in concentrated nitric or HBr acids, where nitrate or bromide anions are complexing enough to form the similar precursor $[Ti(OH)_2X_2(OH_2)_2]$ [10].

The three polymorphs of titania can also be selectively obtained from oxidation of Ti(III) soluble species (acidic media) or solid phases (pH > 3) [11]. In these conditions, the control of the acidity of the medium allows one to control both crystalline structure and morphology of titania nanoparticles (see later). Structural and morphological control of manganese oxides will also be studied in the following. The chemistry of iron oxides is presented elsewhere [12].

4. Control of morphology and shape of oxide nanoparticles

Particle morphology is very often strongly dependent on the crystalline structure of the material, because growth is imposed by the symmetry and the dimensionality of the structure. For instance, spinel iron oxides have a structure based on a face centered cubic stacking of oxide ions in which tetrahedral and octahedral sites are occupied by metal cations (space group Fd3m). The cubic symmetry of the structure well corresponds to pseudo-spherical nanoparticles and to truncated cubes leading to octahedra for large crystal (Fig. 3). Haematite (R-3c) preferentially forms rhombohedral nanocrystals while goethite (Pnma) forms elongated nanorods corresponding well to the preferential growth of crystals along the direction of double chains of octahedra.

The polymorphs of titania present also typical morphologies: octahedral macrocrystals and spherical nanoparticles of anatase ($I4_1/amd$), platelets of brookite (Pcab), needles or rods of rutile ($P4_2/mnm$) (Fig. 4) in

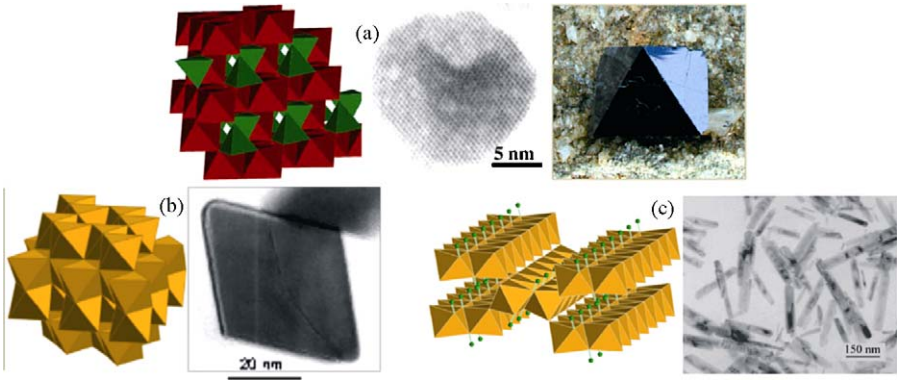

Fig. 3. Crystalline structures and morphologies of particles of (a) magnetite Fe_3O_4, (b) haematite α-Fe_2O_3 and (c) goethite α-FeOOH.

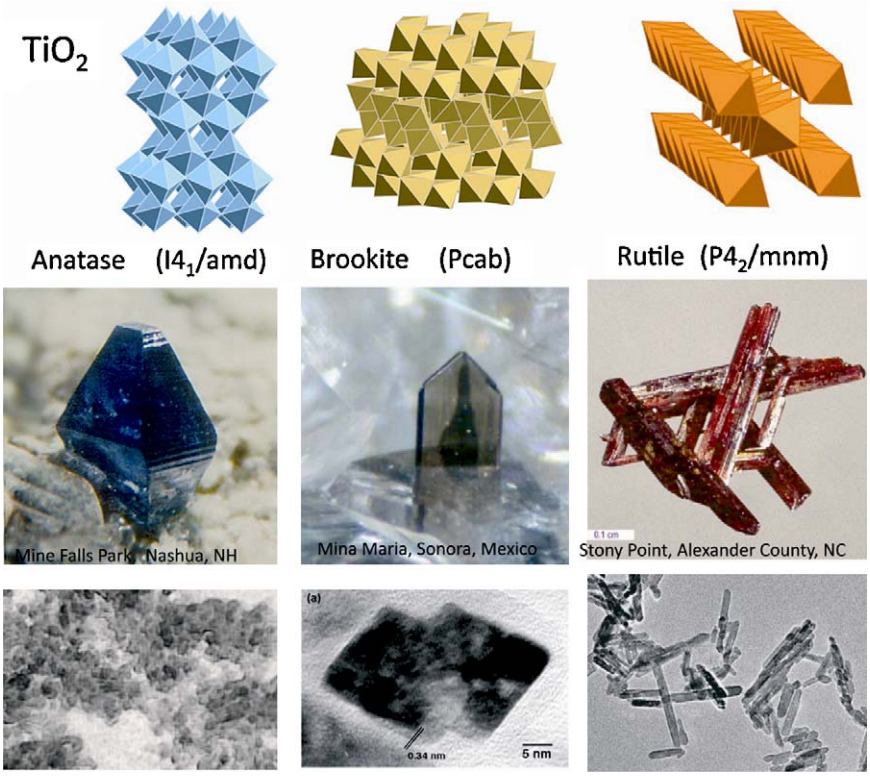

Fig. 4. Crystalline structures and morphologies of natural crystals and nanoparticles of the different polymorphs of titania.

accordance with the crystalline symmetry. Bidimensional structures such as brucite $Mg(OH)_2$ (P-3m1) and boehmite γ-AlOOH (A21am) always forms platelets.

All these particle shapes can be qualitatively explained by the minimization of the total surface energy (Gibbs-Wulf's construction) taking into account the relative values of the interfacial tension of crystal facets. In the case of anisotropic crystalline structure, each facet has its own structure and its own energy. For instance, calculated interfacial energies for boehmite are 0.465 Jm^{-2} for basal faces (010) and 0.600, 0.750, 0.825 Jm^{-2} for (001), (100), (101) lateral faces, respectively, of platelets [3]. That shows that basal faces with the less energy are preferentially developed in comparison to lateral faces. The ''standard'' shape of particles can however be modified and designed for a given application or use, and diverse methods can be used. As for structural control, the adjustment of physicochemical conditions of the medium allows one to control the particle growth process. Modification of particle shape and texture can be obtain through different effects such as adsorption, control of growth kinetic steps and oriented attachment (controlled aggregation).

4.1. Effect of adsorption on particle morphology

As shown before, the exposed faces of particles may not have the same structure and consequently the same physicochemistry and reactivity. It can be interesting to synthesize particles in conditions allowing one to develop specifically some faces. That is typically the case of boehmite nanoparticles, which are used as precursor of γ-alumina, for catalysis. The boehmite → γ-alumina thermal transformation is topotactic and the shape control of boehmite nanoparticles enables one to control the reactivity of alumina.

Boehmite is synthesized by thermolysis at 95 °C of aluminum nitrate in aqueous solution but the morphology and size of nanoparticles are strongly dependent on the pH of the medium. Electron microscopy and X-ray diffraction showed that platelets with different extension of lateral faces are so obtained at different pH and consequently with different surface charge densities (Fig. 5).

Modeling of influence of proton adsorption on the interfacial tension (see part 1) for various crystalline faces of boehmite allows one to account well for these changes in morphology [3,13].

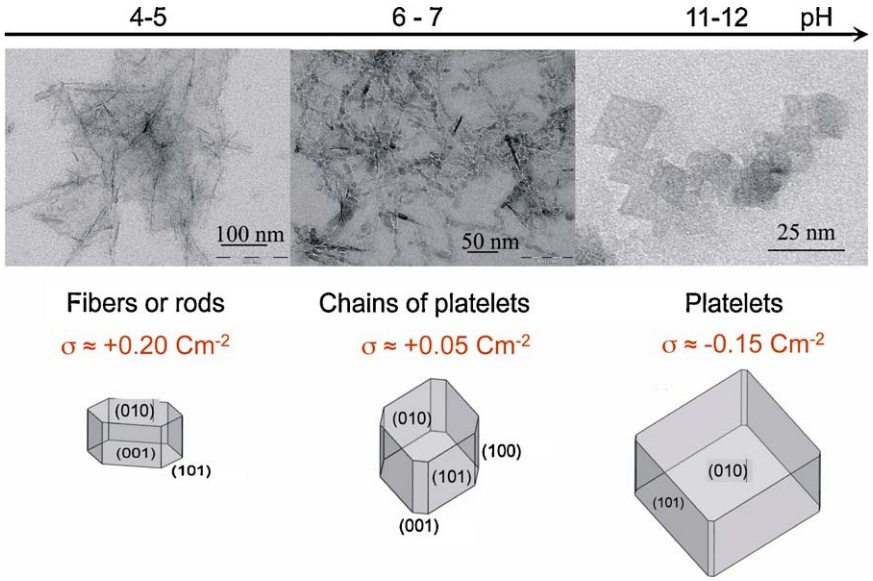

Fig. 5. Electron micrographs of γ-AlOOH boehmite nanoparticles obtained at different pH and corresponding morphologies deduced from the simulation of X-ray diffraction patterns [3,13].

The particle shape of boehmite nanoparticles may also be varied by adsorption of organic molecules, polyols and carboxylic acids of different sizes, conformation and functionalities. The most prominent effects are obtained with molecules having a structural adequacy with the surface giving high adsorption energy [14].

4.2. *Effect of a multistep growth on particle morphology*

The chemistry of manganese dioxide gives rise to very beautiful examples of morphological and textural control based on the rate of formation of the precursor in solution. As there does not exist aqueous soluble complexes of Mn(IV) precursors of manganese dioxides, a classical synthesis of these materials involves redox reactions: reduction of permanganate or oxidation of manganeous complexes by adequate reactants. In order to avoid foreign species, a mediamutation reaction between Mn(VII) and Mn(II) complexes is very often used, following the scheme:

$$2[MnO_4]^- + 3[Mn(OH_2)_6]^{2+} \rightarrow 5[Mn(OH)_4(OH_2)_2] + 4H^+ \quad (1)$$

and

$$[Mn(OH)_4(OH_2)_2] \rightarrow MnO_2 + 4H_2O \quad (2)$$

The key parameters of the system are the Mn(VII)/Mn(II) ratio, pH and temperature of thermolysis. All manganese oxides syntheses presented in this article were made with a total concentration in Mn of 0.2 mol.L^{-1} and precipitation was quantitative in every case [15].

With the stoichiometric Mn(VII)/Mn(II) ratio equal to 2/3, thermolysis at 95 °C for seven days forms long needles of cryptomelane, α-MnO_2 when the pH of the medium is kept below 4 and platelets of birnessite, δ-MnO_2, at pH > 6. In fact, birnessite is a mixed valent phase with a composition around $K_{0.3}Mn^{IV}{}_{0.7}Mn^{III}{}_{0.3}O_2$. At pH < 4, a rapid redox reaction between soluble species leads to an amorphous precipitate which evolves in suspension and forms cryptomelane, the most thermodynamically stable phase in these conditions. Its structure displaying 2 × 2 tunnels grows naturally as needles. At pH > 6, manganeous complexes are initially precipitated as pyrochroite, $Mn(OH)_2$, with the lamellar brucite-like structure. Oxidation proceeds in the solid phase producing birnessite with a derived brucite structure in which potassium ions are inserted between the Mn(IV)-Mn(III) sheets (Fig. 6).

In the presence of an excess of permanganate (Mn(VII)/Mn(II) = 20/3), a first rapid redox reaction between Mn(VII) and Mn(II) leads at pH 2 to more or less spherical amorphous aggregates, and platelets of birnessite at pH 11, as before. In both cases, a second step, much more slow, occurs, corresponding to the reduction of the excess of permanganate by water, according to the equation:

$$4[MnO_4]^- + 2H_2O \rightarrow 4[Mn(OH)_4(OH_2)_2] + 4OH^- \quad (3)$$

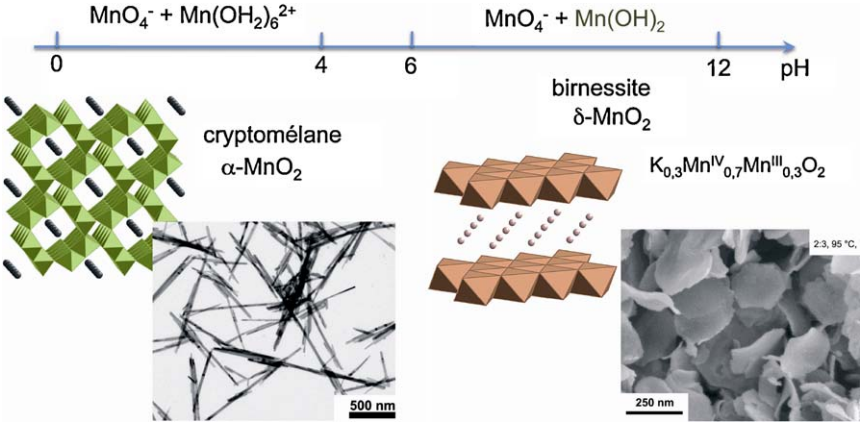

Fig. 6. Crystalline structures and morphologies of MnO_2 particles obtained by thermolysis at 95 °C for 7 days of mixtures of $KMnO_4$ and $MnSO_4$ (Mn(VII)/Mn(II) = 2/3) at different pH [15].

This reaction produces the non-charged complex $[Mn(OH)_4(OH_2)_2]$ and simultaneously provokes the alkalinisation of the medium, so that the complex forms birnessite δ-MnO_2. Because of the slowness of reaction (3), heterogeneous nucleation onto the early particles leads to their decoration. Sponge-like particles are formed as spherical core shell structures with amorphous spherical cores initially produced in an acidic medium [16], and decorated platelets when nucleation occurs onto the platelets formed at initial basic pH [17] (Fig. 7).

In similar conditions, needles of cryptomelane, α-MnO_2 formed with Mn(VII)/Mn(II) = 2/3 (60 °C, pH 2, seven days) can be decorated by birnessite (Fig. 8). Addition of $[MnO_4]^-$ ions into the suspension of needles and heating at 95 °C for one day leads, following reactions, (3) and (2) to heterogeneous nucleation of sheets of birnessite onto the needles. The heteroepitaxy process is allowed by the excellent adequacy between interplanar spacing of (110) planes (d_{110} = 0.69 nm) of cryptomelane and (001) planes (d_{001} = 0.7 nm) of birnessite (misfit of ca. 1%) [18] (Fig. 8).

5. Oriented attachment and particle morphology

Oriented attachment is a mechanism recently recognized to form nanoparticles with sometimes unusual morphologies [19]. That is, for instance, the case for hollow cones made of ramsdellite γ-MnO2 [20] (Fig. 9).

Such particles are still obtained, as before, by mediamutation in $[MnO_4]^-$ and $[Mn(OH_2)_6]^{2+}$ solutions thermolyzed at 95 °C for one day but with the stoichiometric Mn(VII)/Mn(II) ratio equal to 1/4 and initial pH = 9.2, final pH around to 3.7 with a total concentration in manganese of 0.2 mol.L^{-1}. The formation of these particles seems to be rather complex and it is believed to involve many successive steps. In these acidity and composition conditions, the rapid mediamutation reaction forms simultaneously more or less crystalline MnO_2 nuclei. Groutite α-MnOOH nanorods, resulting very likely from hydroxylation and aerial oxidation of the excess of Mn(II) ions are also identified by X-ray diffraction as a transitory species, transforming finally into ramsdellite, an isostructural

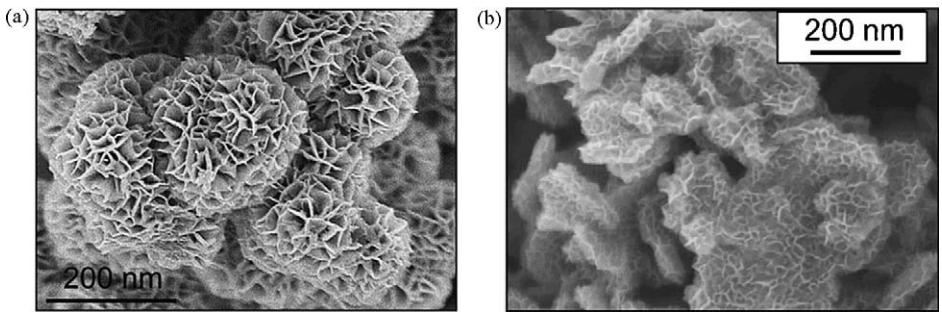

Fig. 7. SEM images of MnO_2 particles obtained after aging 7 days at 95 °C of $KMnO_4$ and $MnSO_4$ mixtures (Mn(VII)/Mn(II) = 20/3) at initial pH 2 (a) and 11 (b) [16,17].

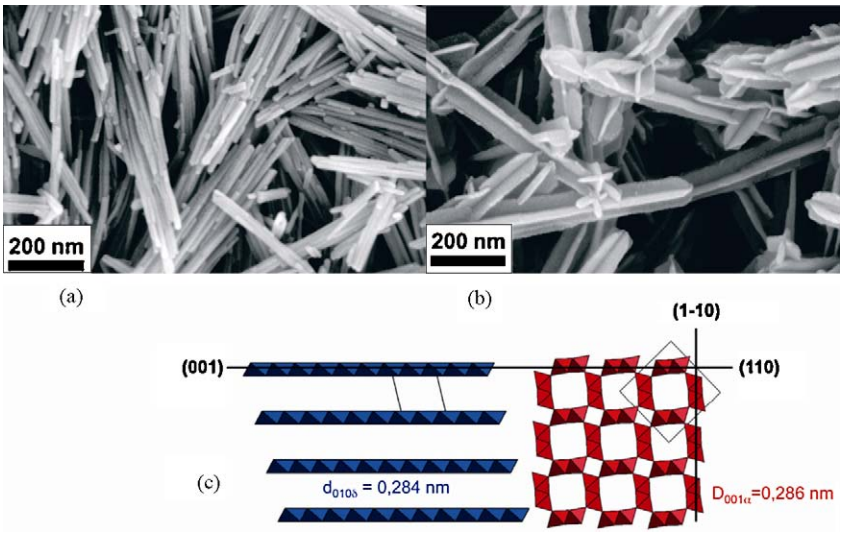

Fig. 8. Field emission scanning electron micrographs of cryptomelane needles (a) and particles decorated by heteroepitaxy of birnessite (b). Structural relation between birnessite and cryptomelane (c) [18].

oxide. Transmission electron images clearly show that the early MnO_2 particles behave as nuclei for ordered aggregation of groutite nanorods. The final shape seems to be resulting from dissolution-crystallization mechanism allowing twinning and smoothing of the six lateral faces of hollow cones (Fig. 10). Precipitation of manganese oxide is quantitative with around 15% in mass of side products, essentially as groutite.

Another unusual morphology generated by oriented aggregation is given by feitknechtite, β-MnOOH, obtained by reduction of $[MnO_4]^-$ ions with thiosulfate $[S_2O_3]^{2-}$ in solution at pH 11 and 60 °C [21] (Fig. 11). The redox conditions correspond to the formation of wires of a Mn(III) compound laterally stacked to form triangles. Here also, a very precisely oriented aggregation and dissolution crystallization are at work to form perfectly twinned and smooth triangles. These particles are, however, metastable and spontaneously transform quasi quantitatively into manganite wires during thermolysis of suspensions.

These last examples, which highlight the complexity and the versatility of the chemistry of manganese in aqueous solution, are interesting because they present two distinct processus involved in the growth of particles: an accumulation of matter from complexes in solution onto a preexistent particle, and the formation of a new particle by aggregation of preformed objects.

6. Design and functionalization of oxide nanoparticles

The aim of functionalization is to adapt nanoparticles to a precise use in various fields of nanotechnologies or to bring them a new property. This may be the adjustment of the size, shape and crystalline structure, as previously described. This concerns also various

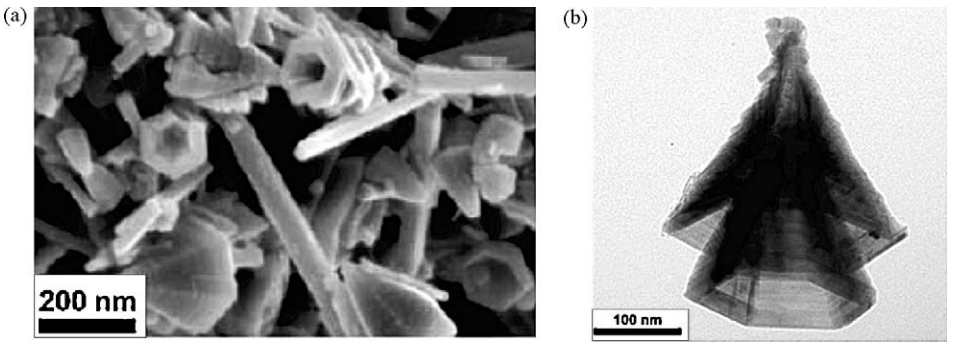

Fig. 9. Field-emission scanning electron micrograph (a) and transmission electron micrograph (b) of cones obtained by thermolysis at 95 °C of $KMnO_4$ and $MnSO_4$ mixtures (Mn(VII)/Mn(II) = 1/4) at initial pH 9.2, final pH around to 3.7 [20].

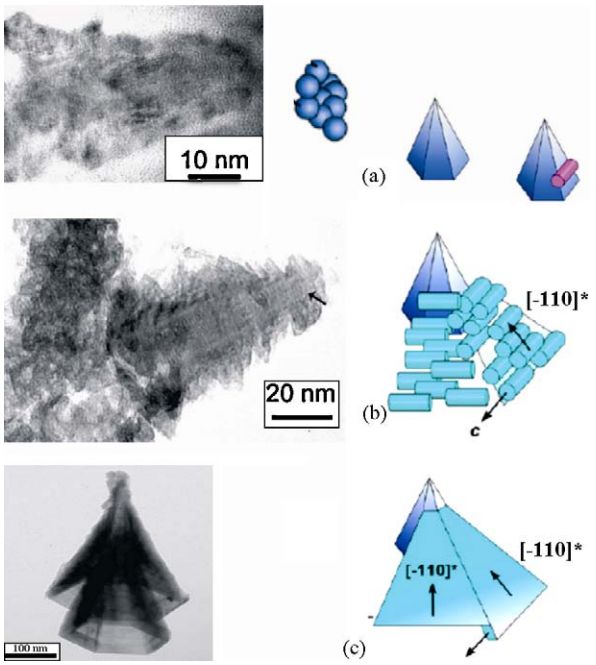

Fig. 10. Possible steps in the formation of ramsdellite γ-MnO_2 hollow cones: crystallization of germs from initial amorphous precipitate (a), attachment of rods of groutite α-MnOOH/ramsdellite resulting from aerial oxidation of the excess of Mn(II) in solution (b), smoothing and twinning of cones by dissolution crystallization [20].

aspects related to surface properties such as dispersability in various media (aqueous or non aqueous), compatibility (to ensure nontoxicity in biological systems and/or furtivity for drug vectors), reactivity (towards adsorption for catalysis or for decontamination of natural or industrial waters, soils...). In this case, functionalization is carried out by a surface treatment or modification of the particles and many strategies can be used, among them the grafting of functional chemical groups or the embedding of nanoparticles by a surface layer to form a core-shell structure. Modifications of the bulk of nanoparticles to obtain, for instance, an optical property (color, luminescence...) may be achieved by a controlled doping made during elaboration of nanoparticles without deep change of the process. We present in the following, examples of these different cases: surface grafting, core-shell structure formation and doping in bulk of silicate nanoparticles.

6.1. Functionalization by surface grafting

Magnetic iron oxide nanoparticles are intensively studied as contrasting agent in resonance magnetic imaging *in vivo* and for drug vectorization. Magnetic properties are specifically involved for guidance and hyperthermia, while nano size allows dispersability and vectorization. However, magnetic nanoparticles have to be functionalized in order to be compatible with the high salinity of the blood in which they are introduced and transported and to avoid to be eliminated in the liver by white corpuscules. Biocompatible polymers such as dextran and polyethylenglycol are adsorbed onto particles to obtain both steric stabilization and furtivity. These polymers are themselves functionalized with folic acidic groups for targeting and various drugs able to be deliver in the proximity of tumoral cells [22].

Colored hybrid coatings with efficient mechanical properties have been elaborated by introducing goethite (α-FeOOH) nanorods and maghemite (γ-Fe_2O_3) nanospheres in a poly(hydroxyethylmethacrylate) (PHEMA) matrix. Both goethite nanorods and maghemite nanospheres lead to a strong reinforcement of the hybrid coatings, even at low volume fraction (4%) [23]. The reinforcement results from a homogeneous dispersion of the particles, which develop strong interactions between the polymer chains and the surface hydroxyl groups of the nanoparticles. In addition to hydrogen bonds, inner coordination complexes between surface iron cation and polymer resulted from hydrolysis of

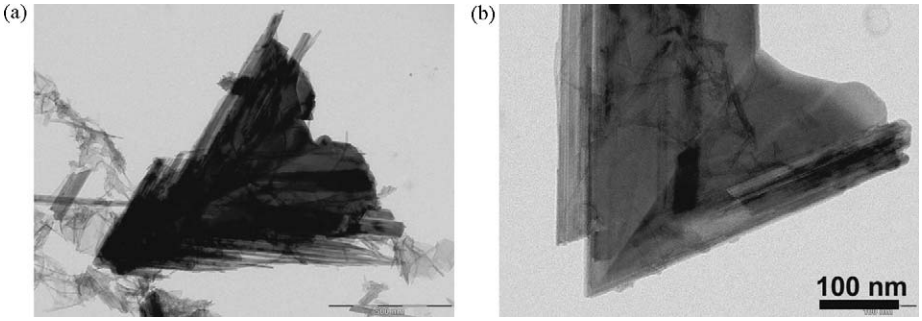

Fig. 11. Transmission electron micrographs of feitknechtite particles obtained by reduction of MnO_4^- by $S_2O_3^{2-}$ (Mn:S = 6) at 60 °C upon 18 hours (a) and two days (b) [21].

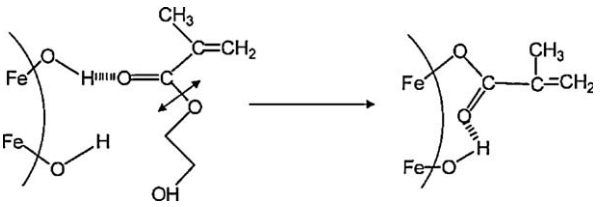

Fig. 12. Scheme of grafting on iron oxide nanoparticle surface of a carboxylate group resulting from hydrolysis of HEMA.

ester functions in PHEMA chains into carboxylate groups (catalyzed by Lewis acidity of Fe^{3+} cations), which grafted of the surface of nanoparticles (Fig. 12). Moreover, the goethite-based hybrid coatings exhibit interesting birefringent properties associated with the stabilization inside the organic matrix of a liquid crystal-type organization resulting from the self-assembly of goethite nanorods. Promising applications of such functional smart coatings are to be expected [23].

6.2. Functionalization by a core-shell structure

Er^{3+}-doped optical fibers are widely used to amplify optical signals in telecommunication systems. New technological developments involve the sensitization of erbium ions by nanoparticles of silicon, resulting from an energy transfer from Si nanoparticles toward Er^{3+} ions. Excitation (pump energy) around 500 nm, mostly absorbed by Si with a large absorption cross-section, is transferred to Er^{3+} ions through the radiative carrier recombination process at 770 nm, enhancing Er photoluminescence at 1550 nm [24]. In order to optimize the phenomenon, we used silicon nanoparticles 7 nm in mean size made by laser pyrolysis [25] which were doped on the surface by Er^{3+} ions. As silicon NP are the most often oxidized on the surface and as this oxidation layer seems to favor photoluminescence, Er^{3+} ions were dispersed into a silica layer deposited onto the nanoparticles. A mixture of Si nanoparticles, tetraethoxysilane ($Si(CH_2CH_3)_4$) and erbium acetylacetonate in ethanol is added under very strong agitation in a solution of ammonia in ethanol. In adequate concentration conditions, heterogeneous nucleation of silica onto silicon take place and forms a shell containing Er^{3+} ions at proximity of silicon. Activation by UV irradiation of the luminescence of the dispersion in alcohol shows the efficiency of the doping method (Fig. 13). Addition of triethoxysilane ($SiHCH_2CH_3)_3$) and acidic water (pH 2) into the dispersion of these core-shell nanoparticles forms a gel. After drying, the material is heated at 800 °C to obtain a

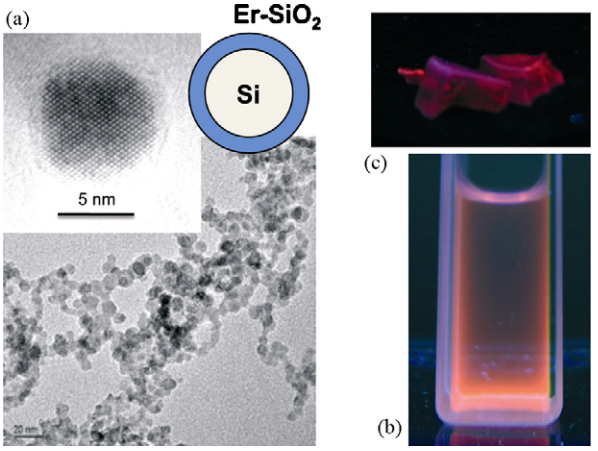

Fig. 13. Transmission electron microscopy images of nanoparticles of silicon embedded in an Er-doped silica shell (a). Luminescence under UV irradiation of these particles in suspensions in alcohol (b) and dispersed in a silica glass (c).

glassy composite in which the doped nanoparticles are trapped (Fig. 13). The thermal treatment avoids fluorescence of silica and allows us to verify that nanoparticles retain their integrity and optical properties in the conditions of fiber elaboration [26].

6.3. Functionalization by doping

A very interesting example of functional nanoparticles is given by nanoprobes with near-infrared persistent luminescence for in vivo imaging [27]. This technology is based on long luminescent nanoparticles emitting in the red to near-infrared range, which can be optically excited before *in vivo* local or systemic injection. The long-lasting persistent luminescence can reach several hours and permits the removal of the background noise originating from *in situ* excitation. Thus, the significant signal-to-noise ratio improvement allows detection in rather deep organs and real-time biodistribution monitoring of active elements during the hours after injection. Rare-earth ions (Eu^{2+}, Dy^{3+}) serve as primary acceptors of the energy (delivered by an UV lamp), which is thermally released to Mn^{2+} ions for several hours. The symmetry and the crystal field strength at the Mn^{2+} site are responsible for an emission in the red and the near-infrared, ($^4T_1 - {}^6A_1$ transition) with maximum intensity around 690 nm.

The main difficulty is the elaboration of nanoparticles (for transport in blood circulation) with the clinoenstatite structure of composition $Ca_{0.2}Zn_{0.9}Mg_{0.9}Si_2O_6$ to optimize emission in the infrared of Mn^{2+} luminescent ions. Eu^{2+}, Dy^{3+} and Mn^{2+} ions were introduced into the aqueous acidic solution of

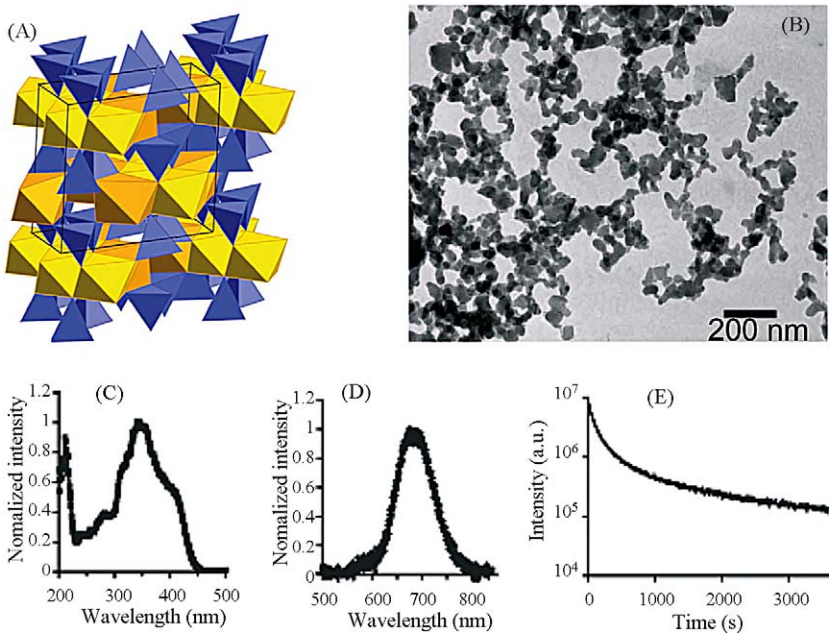

Fig. 14. A. Clinoenstatite structure of $MgSiO_3$. B. Transmission electron microscopy images of the synthesized NPs. C. Excitation spectrum of NPs. D. Long afterglow emission spectrum. E. Time dependence of the luminescence intensity of the NPs. NPs (10 mg) were under direct exposure to a 6-W UV lamp for 5 min. The luminous intensity was quantied straightforward by using an intensied charge-coupled device (ICCD) camera (PhotonImager, Biospace). The luminous decay data were t by a power law function for time > 100 s [27].

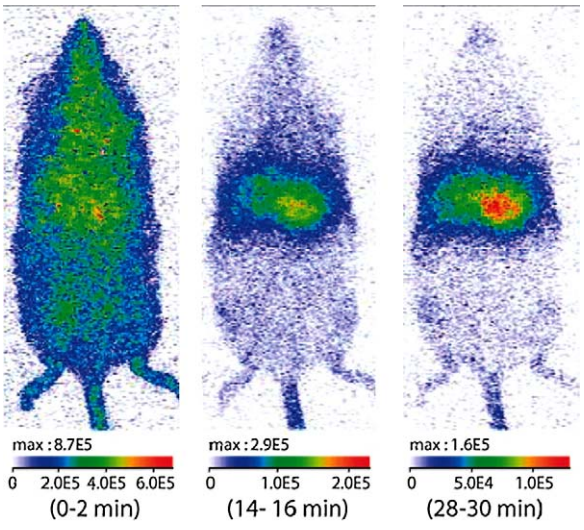

Fig. 15. In vivo biodistristribution of NPs modified in surface by reaction with 3-aminopropyltriethoxysilane and with diglycolic anhydride. Optical imaging of a mouse with 1-mg tail vein injection of NPs. (Preinjection of anionic liposomes slows down the opsonization and improves the circulation duration of NPs.) All images correspond to a 2-min signal acquisition performed between the times indicated below each image. The luminous intensity is expressed in photons per $s.cm^2$.steradians [27].

Ca^{2+}, Zn^{2+} and Mg^{2+} ions, in which was added tetraethoxysilane. Gelification occurred by gentle heating, and after drying, the solid was heated in a slightly reductive atmosphere at 1050 °C for 10 hours. By grinding and selective centrifugation, nanoparticles of 50–60 nm in diameter (Fig. 14) easily dispersible in water were obtained. Of course, nanoparticles were biocompatibilized by a coating of 3-aminopropyltriethoxysilane and polyethylenglycol. The *in vivo* biodistribution of nanoparticles in a Swiss mouse is obtained by detection of the signal with an intensified charge-coupled device (ICCD) camera (Fig. 15) [27].

7. Conclusion

This study focusing on the elaboration of metal oxides nanoparticles from solution, shows through various examples the possibility to produce well-defined and original nanoarchitectures and to ensure the design of nanoparticles. Aqueous chemistry of cations, which is known to be "*douce*" and green, appears also highly versatile, in supposing many parameters of synthesis (composition, acidity, redox conditions, temperature, concentration...) well understood and controlled. Nanoparticles are very well characterized by high-resolution electron microscopy and X-ray

diffraction. However, many other techniques can be used nowadays to probe *in situ* the transformations and to fully understand their mechanisms.

References

[1] Nanosciences - Nanotechnologies. Rapport sur la science et la technologie n° 18 réalisé avec l'Académie des technologies. Avril 2004.

[2] Environmental nanotechnology. Applications and impacts of nanomaterials, in: M. Wiesner, J.Y. Bottero (Eds), Nanomaterials fabrication, in: J.P. Jolivet, A. Barron (Eds), chap. 3, McGraw-Hill, 2007, pp. 29–103.

[3] J.P. Jolivet, C. Froidefond, A. Pottier, C. Chanéac, S. Cassaignon, E. Tronc, P. Euzen, J. Mater. Chem. 14 (2004) 3281.

[4] R. Aveyard, Chem. Ind., 1987, 474 ;
J. Th. G. Overbeek, Faraday Discuss. Chem. Soc. 65 (1978) 7.

[5] J.L. Dormann, D. Fiorani, E. Tronc, Magnetic relaxation in fine-particle systems, in : Advances in Chemical Physics, Wiley, New York, 1997.

[6] A. Pottier, S. Cassaignon, C. Chanéac, F. Villain, E. Tronc, J.P. Jolivet, J. Mater. Chem. 13 (2003) 877.

[7] A. Pottier, C. Chanéac, E. Tronc, L. Mazerolles, J.P. Jolivet, J. Mater. Chem. 11 (2001) 1116.

[8] E. Baudrin, S. Cassaignon, M. Koelsch, J.P. Jolivet, L. Dupont, J.M. Tarascon, Electrochem. Comm. 9 (2) (2007) 337.

[9] A. Dessombz, D. Chiche, P. Davidson, P. Panine, C. Chanéac, J.P. Jolivet, J. Amer. Chem. Soc. 129 (18) (2007) 5904.

[10] S. Cassaignon, M. Koelsch, J.P. Jolivet, J. Mater. Science 42 (16) (2007) 6689.

[11] S. Cassaignon, M. Koelsch, J.P. Jolivet, J. Phys. Chem. Solids 68 (5–6) (2007) 695.

[12] J.P. Jolivet, C. Chanéac, E. Tronc, Chem Comm. (2004) 481.

[13] D. Chiche, M. Digne, R. Revel, C. Chanéac and J.P. Jolivet, J. Phys. Chem. C 2008, 112, 8524.

[14] Size and shape control of boehmite nanoparticles, a precursor of gamma-alumina catalyst, in: D. Chiche, C. Chanéac, R. Revel, J.P. Jolivet (Eds), Scientific Bases for the Preparation of Heterogeneous Catalysts, E.M. Gaigneaux, et al. (Eds), Studies in Surface Sci. and Catalysis, vol. 162, Elsevier, 2006, pp. 393–400.

[15] D Portehault, S. Cassaignon, E. Baudrin, J.P. Jolivet, J. Mater. Chem, 2009, DOI: 10.1039/B816348K.

[16] D. Portehault, S. Cassaignon, N. Nassif, E. Baudrin, J.P. Jolivet, Angew. Chem. Int. Ed. 47 (2008) 6441.

[17] D. Portehault, S. Cassaignon, E. Baudrin, J.P. Jolivet, Chem. Mater. 20 (19) (2008) 6140.

[18] D. Portehault, S. Cassaignon, E. Baudrin, J.P. Jolivet, Chem. Commun. (2009) 674.

[19] H. Cölfen, M. Antonietti, Mesocrystals and Nonclassical Crystallization, Wiley, Chichester, 2008.

[20] D. Portehault, S. Cassaignon, E. Baudrin, J.P. Jolivet, Cryst. Growth Design. 9 (2009) 2562.

[21] D. Portehault, S. Cassaignon, E. Baudrin, J.P. Jolivet, Cryst. Growth Design, 2009, Submitted.

[22] S. Mornet, S. Vasseur, F. Grasset, E. Duguet, J. Mater. Chem. 14 (2004) 2161.

[23] N. Chemin, L. Rozes, C. Chanéac, S. Cassaignon, E. Le Bourhis, J.P. Jolivet, O. Spalla, E. Barthel, C. Sanchez, Chem. Mater. 2008, 20, 4602.

[24] S. Moon, B. Hyeon Kim, P.R. Watekar, W.T. Han, J. Non-Crystalline Solids 353 (2007) 2949.

[25] Laser synthesis of nanosized powders, in: M. Cauchetier, E. Musset, M. Luce, N. Herlin, X. Armand, M. Mayne (Eds), Nanostructured silicon based powders and composites, in: A.P. Legrand, C. Senemaud (Eds), Routledge, UK, 2003, pp. 6–24.

[26] Optical guide comprising nanoparticles and method of producing a preform which is intented to form one such optical guide, in: A. Pastouret, S. Blanchandin, C. Chanéac, S. de Monredon, J.P. Jolivet (Eds), Intern. Patent, WO 2007-020362, WO 2006-FR50802, 17/08/2006.

[27] Q. le Masne de Chermont, C. Chanéac, J. Seguin, F. Pellé, S. Maîtrejean, J.P. Jolivet, D. Gourier, M. Bessodes and D. Scherman. Nanoprobes with near-infrared persistent luminescence for in vivo imaging. PNAS 2007, 104, 9266.